Analysis and Testing of a Composite Fuselage Shield for Open Rotor Engine Blade-Out Protection

J. Michael Pereira[1], William Emmerling[2], Silvia Seng[3],
Charles Frankenberger[3], Charles R. Ruggeri[1],
Duane M. Revilock[1], Kelly S. Carney[4]

[1] *NASA Glenn Research Center, Cleveland, OH*
[2] *FAA William J. Hughes Technical Center, Atlantic City, NJ*
[3] *Naval Air Warfare Center, China Lake, CA*
[4] *George Mason University, Fairfax, VA (NASA Retired)*

Abstract

The Federal Aviation Administration is working with the European Aviation Safety Agency to determine the certification base for proposed new engines that would not have a containment structure on large commercial aircraft. Equivalent safety to the current fleet is desired by the regulators, which means that loss of a single fan blade will not cause hazard to the Aircraft. The NASA Glenn Research Center and The Naval Air Warfare Center (NAWC), China Lake, collaborated with the FAA Aircraft Catastrophic Failure Prevention Program to design and test lightweight composite shields for protection of the aircraft passengers and critical systems from a released blade that could impact the fuselage. LS-DYNA® was used to predict the thickness of the composite shield required to prevent blade penetration. In the test, two composite blades were pyrotechnically released from a running engine, each impacting a composite shield with a different thickness. The thinner shield was penetrated by the blade and the thicker shield prevented penetration. This was consistent with pre-test LS-DYNA predictions. This paper documents the analysis conducted to predict the required thickness of a composite shield, the live fire test from the full scale rig at NAWC China Lake and describes the damage to the shields as well as instrumentation results.

Introduction

The Federal Aviation Administration is working with the European Aviation Safety Agency to determine the certification base for proposed new engines that would not have a containment structure on large commercial aircraft. Equivalent safety to the current fleet is desired by the regulators, which means that loss of a single fan blade will not cause hazard to the Aircraft. The NASA Glenn Research Center and The Naval Air Warfare Center (NAWC), China Lake, collaborated with the FAA Aircraft Catastrophic Failure Prevention Program to design and test lightweight composite shields for protection of the aircraft passengers and critical systems from a released blade that could impact the fuselage. The effort involved both computational analyses and experimental verification. In the computational analyses the geometry of a test setup was designed in such a way that a released blade would impact a fuselage shield in the worst case configuration, and predictions were made for the required thickness of a composite shield to prevent penetration of a representative blade (Ref. 1). For the experimental verification, a full scale test was conducted in which two composite blades were released from a running engine in such a way that each impacted a composite shield of differing thickness in the predicted worst case configuration (Ref. 2).

Geometry

A medium-range, twin-engine, narrow-body jet airliner served as the basis for the notional open-rotor aircraft. The geometry assumptions, shown in Figure 1, were obtained from the FAA-directed, NAWC Open-rotor Analysis (Ref. 3). The horizontal distance from the centerline of the fuselage to the centerline of the engine is approximately 188 inches (BL or Butt Line axis). The vertical distance from the centerline of the fuselage to the center line of the engine is approximately 85 inches (WL or Water Line axis). The diameter of the engine hub was assumed to be approximately 78.5 inches, and with the length of each blade being approximately 41.28 inches. The overall open-rotor engine diameter is approximately 161 inches.

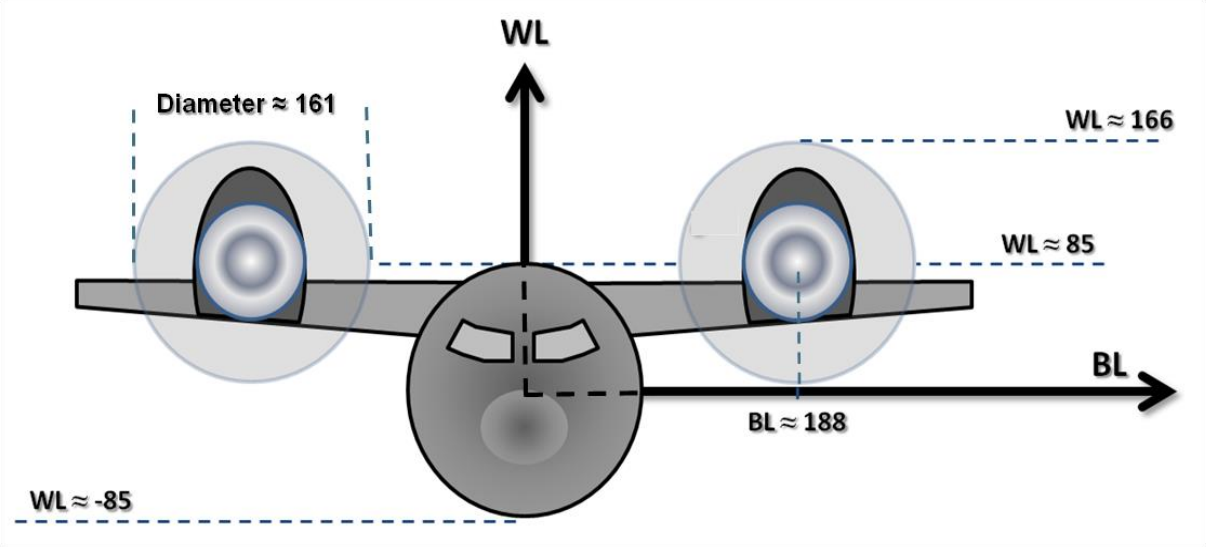

Figure 1. High Wing Mounted Open-rotor Study Airframe Geometry.

The blades used for analysis and testing were similar in design and materials to those that could be used for open rotor engines. A modern propeller was used as the surrogate with the outer portion acting as the released open rotor simulation. The blades have a polyurethane foam core, sandwiched between carbon fiber spars, with composite reinforced skins. A thin strip of nickel protects the leading edge from small, "nominal," foreign object damage, such as small debris from unimproved runways (Figure 2).

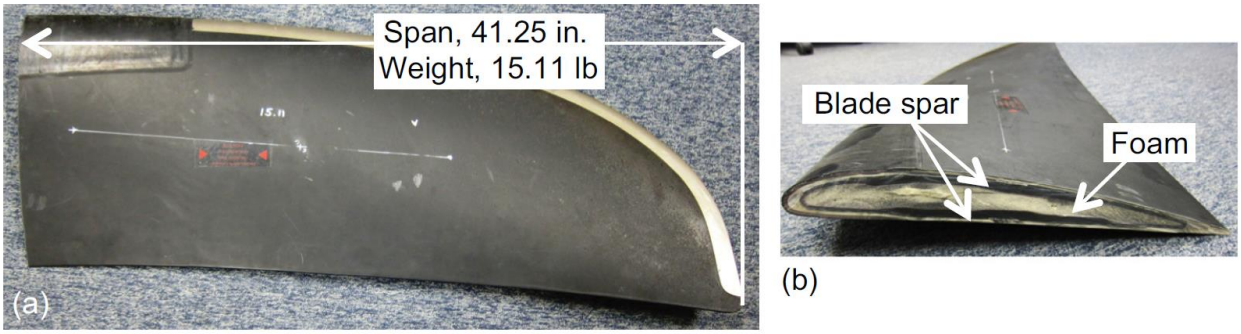

Figure 2. Outer section of blade used for analysis and full scale testing. (a) Section length and weight. (b) Blade cross section.

Experimental Design

The shielding concept being investigated incorporates composite shields placed around the perimeter, or a portion of the perimeter, of the fuselage adjacent to the blade plane of rotation. A trajectory study based on the aircraft geometry in Figure 1 was conducted to determine the worst-case angle and velocity for the impact analysis (Ref. 1). The results from the trajectory study were then used as initial conditions for the impact analysis. The blade could then be placed close to the fuselage at the beginning of the impact analyses to minimize the computational run times. The worst case situation was considered to be when the long axis of the blade was parallel to the blade linear velocity and normal to the tangent of the curved fuselage shield at the impact point.

Based on the trajectory analysis a test geometry was designed that would allow two blades rotating on an engine to be simultaneously released and impact shields in what was considered the worst case situation. The objective was to have a 41.25-inch-long blade section, weighing 15.1 lb., impact the shield at a velocity of 527 ft./sec. The geometry of the test setup is shown in Figure 3. To achieve the desired conditions a blade release angle of 8 degrees was selected.

Pre-test Impact Analysis

For the impact analyses, a triaxially-braided composite comprising TORAYCA T700S fibers and CYCOM PR520 toughened resin was selected for both the shield and the blade. The braid architecture was composed of 24k tows in the 0º direction and 12k tows in the ±60º directions with the same fiber volume in each direction so that the in-plane stiffness properties were quasi-isotropic. Considerable mechanical property and impact test data, as well as analytical material modeling results are available for this material (Refs. 4 to 8). The mechanical property test results, which were used to populate the LS-DYNA® model of the T700S/PR520, are shown in Table 1, as well as the sources for the data.

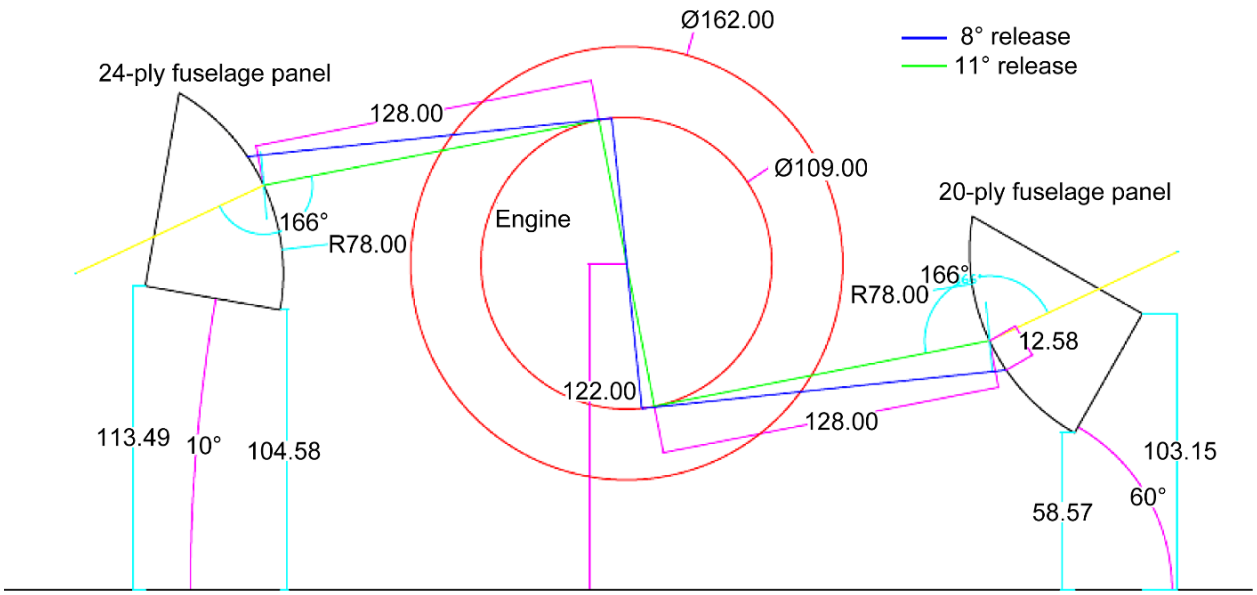

Figure 3. Engine and shield panel setup based on the trajectory analysis. Two blade release angles are shown.

Table 1. Properties Used in the T700S/PR520 Material Model

Material Property	**Value**	**Source**
Density	0.0645 lbs/in^3	Ref. 8
Young's Modulus – Longitudinal	6.904E+06 lbs/in^2	Ref. 4
Young's Modulus – Transverse	6.092E+06 lbs/in^2	Ref. 4
Poisson's Ratio	.31	Ref. 5
Shear Modulus – In-plane	5.062E+06 lbs/in^2	Ref. 4
Shear Modulus – Out-of-plane	2.214E+05 lbs/in^2	Ref. 4
Strain at Longitudinal Compressive Strength	0.018	Ref. 5
Strain at Longitudinal Tensile Strength	0.021	Ref. 6
Strain at Transverse Compressive Strength	0.012	Ref. 5
Strain at Transverse Tensile Strength	0.021	Ref. 7
Strain at Shear Strength	0.011	Ref. 5
Longitudinal Compressive Strength	5.329E+04 lbs/in^2	Ref. 6
Longitudinal Tensile Strength	1.418E+05 lbs/in^2	Ref. 6
Transverse Compressive Strength	4.663E+04 lbs/in^2	Ref. 6
Transverse Tensile Strength	1.418E+05 lbs/in^2	Ref. 6
Shear Strength	4.596E+04 lbs/in^2	Ref. 6

To model the impact of the blade on the composite shield LS-DYNA Rate Sensitive Composite Fabric, MAT158, was used. This material model is based on Schweizerhof's (Ref. 9) implementation of Matzenmiller's (Ref. 10) theoretical approach. This approach is a continuum damage model, and includes damage parameters which control the non-linearity of the stress-strain curve. In Schweizerhof's implementation, there are three damage parameters (one for each of the two orthogonal directions, and one for shear), which are initially set to 0. Each integration layer in the composite has its own set of damage parameters. As strain increases, and one of the

parameters in an individual shell integration layer reaches 1, failure occurs, and the element can no longer take load.

Several different approaches may be taken in the use of MAT158 to model composites. The modeling approach used with MAT158 in this study was the homogeneous approach, where a single set of input parameters describes the composite material. In this model strain rate effects are included by the addition of a viscous stress tensor, which is based on an isotropic Maxwell model with terms in a Prony series expansion. The terms are superimposed on the rate independent stress tensor of the composite fabric, and so are quasi-isotropic. Since the braided composite system used in this study is also quasi-isotropic, this viscoelastic representation of strain rate effects is acceptable. The terms are defined as a shear relaxation modulus and a shear decay constant, and must be determined by analytical trial and error. The terms used in this study are shown in Table 2 which is based on extrapolating data obtained at a series of lower strain rates (Ref. 1).

Table 2. Prony Series for Modeling Rate Effects

Shear Relaxation Term	Shear Decay Constant
3.0E+05	1.0
1.5E+05	10.0
1.5E+05	1000.0
1.5E+05	100000.0

The input parameters for the Rate Sensitive Composite Fabric material model in LS-DYNA were created from the information in Tables 1 and 2. The failure surface type was defined as faceted (FS = -1). All of the factors to determine the minimum stress limit after stress maximum (SLIMs) were set to 1.

The element erosion criteria associated with the composite material model was calibrated by comparisons to a series of ballistic impact tests on flat composite panels of the same material used in this study (Ref. 7).

The interior of the surrogate blade consists of a foam core. For this analysis, a low-density, closed-cell foam, identified as PDL, was used for the blade core. (PDL was an acronym for the (since defunct) Polymer Development Laboratory, an early supplier.) PDL was selected because a validated foam material model was available from the Space Shuttle Program (Ref. 11). A previously created stainless steel material model was used for the metallic leading edge guard (Ref. 12).

A finite element mesh was created from the outer surface blade geometry. Since only the outer surface was available, and detailed drawings and geometry files of the surrogate blade interior were not available, the internal structure used for the finite element model was approximated, and does not represent an actual blade. Nevertheless, an attempt was made to adhere as much as possible to the surrogate blade during the finite element model creation, including a foam core and a composite shell and spar. The foam core of solid elements was covered by a set of shell elements representing the braided composites. For all shell elements, the node locations were

defined to be the top surface of the element. By defining the nodes this way, correct blade thicknesses and center of inertias were properly defined. The same nominal mesh size (0.2 inches) used in the calibration analysis on the flat plates was maintained for this study. Element sizes deviate from the nominal 0.2 inches locally due to the complex blade geometry.

The geometry of the study fuselage was based upon that of a medium-size airliner, with an elliptical shape and a major axis (height) of 157.87 inches and a minor axis (width) of 148 inches. The same mesh size (0.2 inches) used in the material model impact analysis correlation and validation was used for the fuselage shielding mesh. This consistency is important for the validity of the onset of element erosion prediction. In order to reduce run times, only a 45-degree segment (59.2 inches arc length) of the fuselage shielding was included in the impact analysis, as shown in Figure 4. The fuselage shielding was 24 inches wide. Simply supported boundary conditions were enforced at the edges of the shielding.

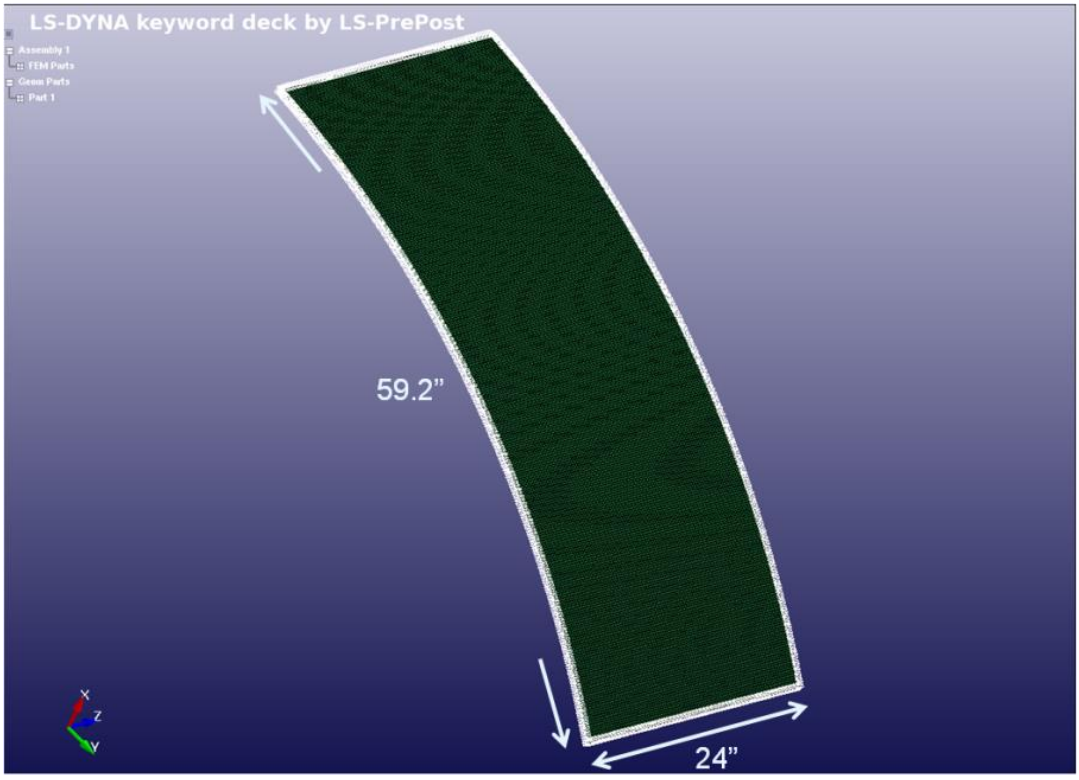

Figure 4. Fuselage Shielding Finite Element Mesh.

Impact Analysis Results

As mentioned above, the initial conditions of impact velocity and blade orientation for the impact simulation were obtained from the trajectory study. This initial position is shown in Figure 5. As stated previously, the initial impact velocity was 509.7 ft/sec perpendicular to the fuselage skin at the impact location. The orientation of the blade was blade tip first; with the velocity vector pointed straight in. The blade also has an initial rotational velocity.

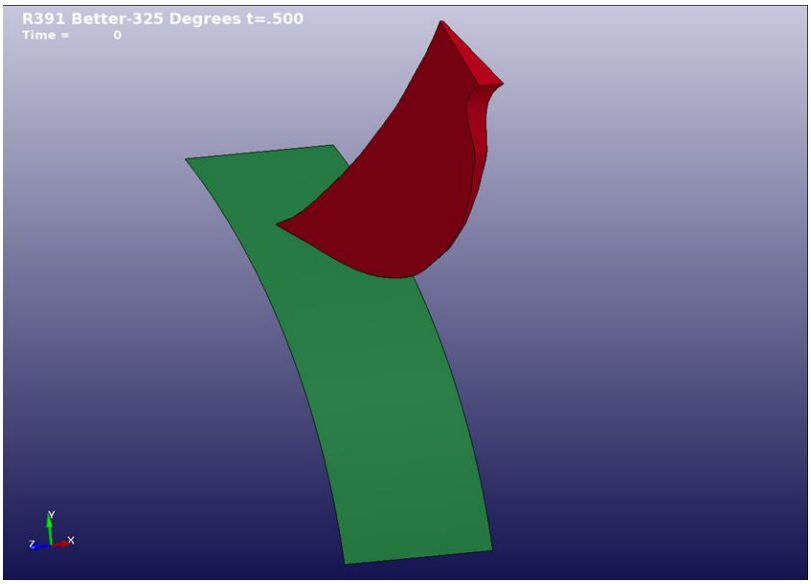

Figure 5. Impact Analysis Initial Position.

Several fuselage thicknesses less than 0.458 inches were analyzed and were found to provide inadequate shielding to prevent blade penetration. For shielding with a thickness of .458 inches (22 composite layers) the blade fails the fuselage surface but does not penetrate into the cabin. Just after initial contact, the blade tip elements fail while the fuselage is stressed below its failure limit. As the rest of the blade continues traveling toward the fuselage, the spar contacts the fuselage causing the shielding to fail. The spar, which is stronger and more massive than the blade tip, is what fails the shielding in the analysis prediction. When the thickness of the shielding was increased to 0.500 inches (24 composite layers), the fuselage shielding was predicted to remain intact, with no breach of the skin and no element erosion. No attempt was made to further refine the required thickness calculations beyond the 0.458 inches that failed, and the 0.500 inches that prevented penetration.

Full Scale Verification Test

The verification test involved releasing two rotating composite blades from a spinning engine such that they impacted two composite shields of different thicknesses at the desired velocity and orientation.

The composite fuselage panels manufactured for the full scale test were based on the results of the pre-test impact analyses. The panels did not contain any stiffeners or stringers. The design concept for the shielding was a floating panel that would not be subject to the flexure of the primary aircraft structure. By isolating the panel from the fuselage structure, the panel is not exposed to the additional stresses and strains and can be made of a lighter-weight material than a structural shielding panel.

Each composite test panel was a 4 ft. x 8 ft. section with a radius of curvature of 6.5 ft. Two composite panels were fabricated, one composed of 20 layers of braided carbon fiber pre-preg, resulting in a thickness of approximately 0.45 inches, and one composed of 24 layers, resulting in a thickness of approximately 0.56 inches. The pre-preg consisted of a triaxially braided

carbon fiber (T700S) braid from A&P Technology (Cincinnati, OH) and Cytec MTM45-1 resin. This resin was chosen because it provides a high strength, damage-resistant, structural epoxy matrix that can be processed in an autoclave without expensive tooling, and was similar to the PR520 used in the analysis. The specifications for the material are shown in Table 3.

Table 3. Composite material specifications

Preform (Triaxially braided flat fabric)	
A&P Product code	QISO-H-52.8-A
Width	52.8 in
Fiber areal weight	536 gsm
Fiber Orientation	0° +/- 60°
Directional content	33.3% in each orientation
Fiber type	T700SC-12K50C
Prepreg (Cytec MTM45-1/QISO-H-52.8-36%RW 52.8" width)	
Resin	MTM45-1
Resin content	36 wt %
Width	52.8 inch
Process method	Dual film
Standard Operating Conditions (SOC)	SOC document to be provided after processing conditions are locked in duriung initial trials

The panel was supported in a frame that matched the boundary conditions in the analysis as much as possible. The panel mounting structure was designed to simply support the panel in the three translational directions, allowing rotation along the panel edges. Details of the mounting structure are given in Reference 2.

The blades used for this testing were similar in design and materials to those that could be used for open rotor engines. A modern propeller was used as the surrogate with the outer portion acting as the released open rotor simulation (Figure 2).

A single test event was conducted. Two blades were mounted to a rotor hub on the Naval Air Warfare Center spin fixture as shown in Figure 6. The spin fixture is a T406 engine and gearbox that are capable of providing 1108 rpm speed required for this test. The two blades were explosively released at 8 degrees past vertical. Two 4 ft x 8 ft composite panels were located approximately 124” from either side of the centerline of the spin fixture such that they were centered on the predicted blade release trajectories. Fuselage structure was not represented.

Figure 6. Blades mounted on the spin fixture. Test panels are shown on either side of the fixture.

Linear shape charges were placed 41.25 inches from the blade tip of each of the blades. The shape charges were simultaneously initiated to release the blades at the same time.

Three pairs of high speed digital video cameras were utilized to quantitatively measure the full field deflection of the backside of each of the test panels as well as the kinematics of one of the released fan blades. The commercial Digital Image Correlation software ARAMIS (GOM mbH, Braunschweig, Germany) was used to compute the 3D panel deflections and in-plane strains based on images obtained from a calibrated pair of cameras focused on the backside of each panel. The panels were painted with .625 in diameter black dots, on one inch centers, on a white background. For the 20 ply panel a pair of Photron model SA5 cameras (Photron USA, San Diego, CA) were mounted on a tripod behind the panel in such a way that the whole panel was visible. These cameras had a resolution of 832 pixels along the length of the panel and 600 pixels across the width, a frame rate of 15000 frames/sec and an aperture time of 1/59000 sec. For the 24 play panel a pair of Photron model SA1.1 cameras was used, in a similar configuration. The camera resolution along the length of the panel was 704 pixels and 448 pixels across the width. The frame rate was 18000 frames per second and the aperture time was 1/49000 sec. The system used on the 24 ply panel is shown in Figure 7

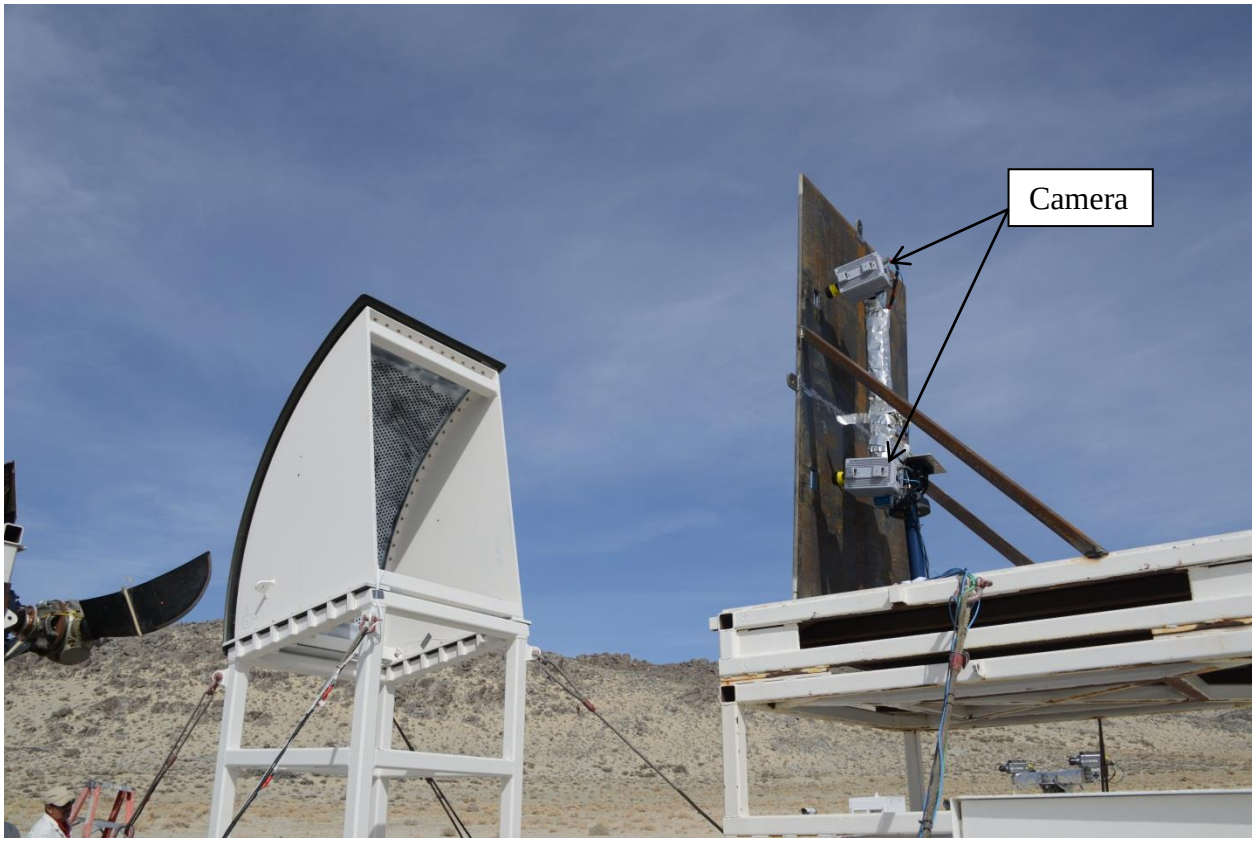

Figure 7. Photogrammetry camera setup for the 24 ply panel

To measure the kinematics of the blade impacting the 20 ply panel, the commercial software PONTOS (GOM mbH, Braunschweig, Germany) was used in conjunction with a pair of Phantom V7.3 cameras (Vision Research Inc., Wayne, NJ). The camera pair was mounted forward and to the right of the engine axis viewing the area from the blade release to the panel impact. These cameras had a frame rate of 12500 frames/sec, a horizontal resolution of 768 pixels, a vertical resolution of 504 pixels and an exposure time of 20 microseconds. Figure 8 shows the camera pair location relative to the test hardware and figure 9 shows a representative frame from the video after blade release and prior to impact. The white dots on the blade and the test article were individually tracked in order to obtain blade linear and angular velocity during the test. However, due to the large amount of light generated from the explosive charges used to release the fan blades and the resulting over-exposure of the images, only a portion of the free flight of the blade segment could be tracked.
Accelerometers were mounted on the panel fixture at strategic locations to measure frame movement during the impact event.

Figure 8. Cameras used for Measuring Blade Kinematics

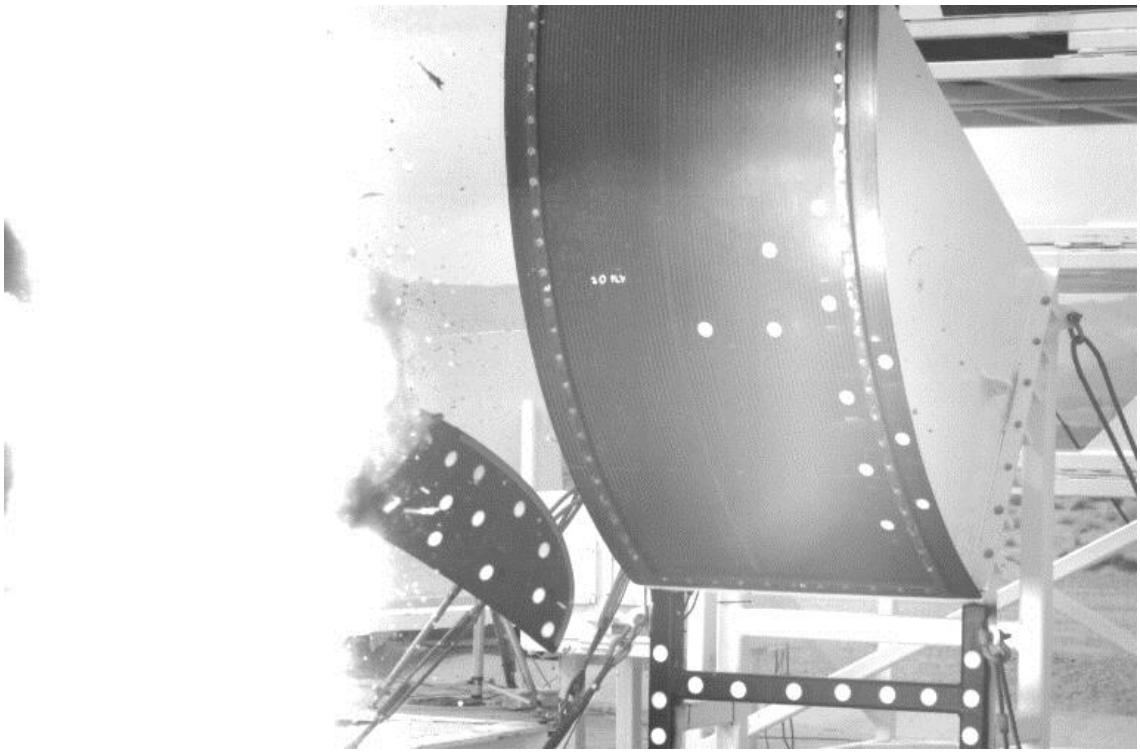

Figure 9. Still Image from one of the video cameras used to track the blade

Full Scale Test Results

Testing was conducted on February 20, 2014. All test systems functioned nominally and the blades were released as intended, at 8 degrees past vertical (Figure 10). The test conditions are noted in Table 4, below. The blades separated as intended and struck the composite test panels. Figure 10 shows a composite photograph of the release of the blades just before shape charge detonation, just after the shape charges were fired, and at first impact of the blades against the composite panels. The upper blade impacted the 24-ply panel and resulted in a large crack but no penetration. The lower blade impacted the 20-ply panel and, as predicted, penetrated the panel. The test results showed good correlation to the pre-test impact analysis.

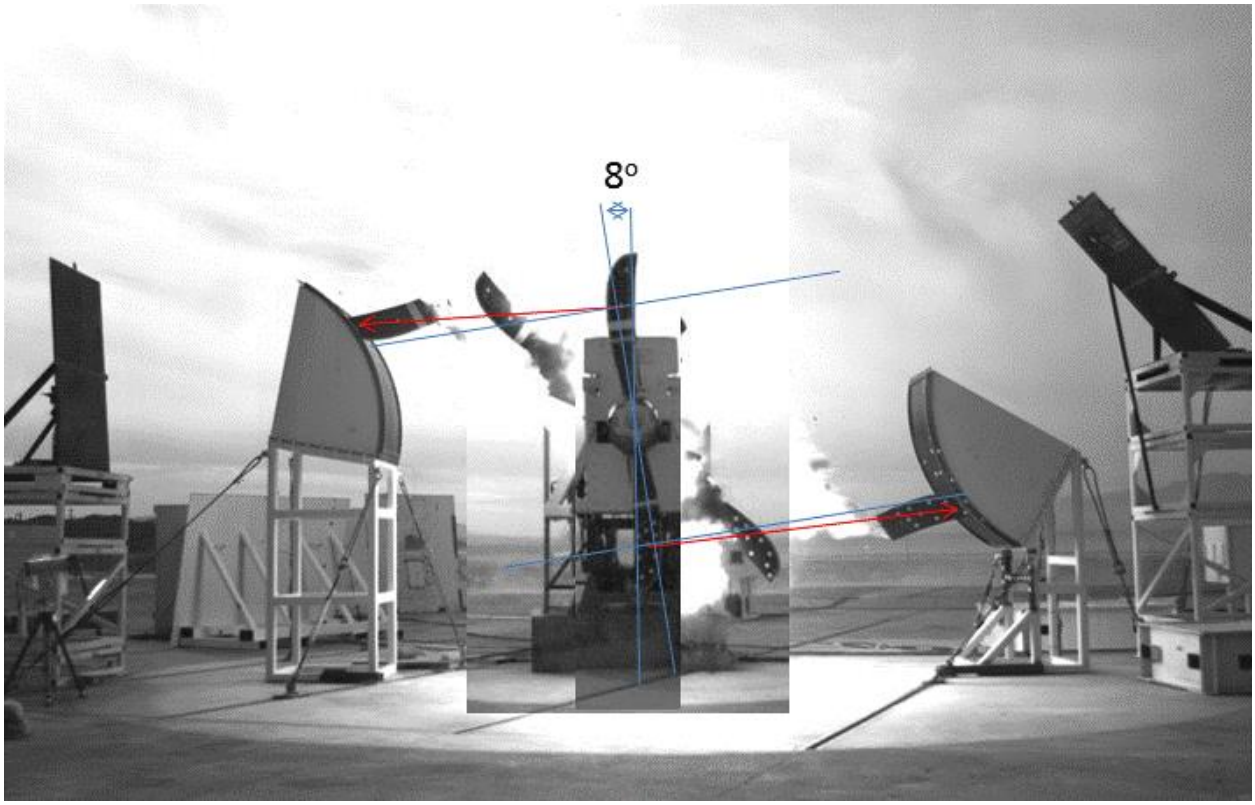

Figure 10. Composite Photograph of Blade Release with Release Angles

Table 4. Test Conditions

Test Condition	Desired (Upper/Lower Panel)	Actual (Upper/Lower Panel)
Blade Release Position	188º/8º	188º/8º
Blade Velocity	1108 RPM	1120 RPM
Blade Release Velocity	527 ft/s	533 ft/s
Blade Weight	15.1 lb.	
Distance of Blade Impact (forward of plane of rotation)	5 in	12.5 in/11.5 in
Blade Kinetic Energy	68657.41	67188.32
20-ply Panel Thickness		0.452 in
24-ply Panel Thickness		0.560 in

Additional analysis was conducted to estimate the test impact condition. Blade release velocity was analyzed by reviewing high speed video and calculating velocity from engine RPM. The geometry of the test and timing from the high speed video provided a calculated blade fragment velocity of 534 feet/second. A second calculation was conducted based on propeller speed (RPM) and estimated blade fragment center of gravity radius of 54.5 inches. This calculation resulted in a blade velocity of 533 feet per second.

The 20 ply panel was impacted by the lower blade with a blade release angle of 188º. The blade released cleanly from the hub and rotated about the center of gravity of the released fragment. The trajectory of the blade was approximately 4º above horizontal. The blade impacted tip first, with the length of the blade along the velocity vector. The blade caused a large tear in the panel, approximately 45" vertically and 12 inches horizontally, and penetrated completely. Two additional horizontal cracks caused delamination but did not penetrate the full thickness of the composite. After passing through the panel, the blade impacted the mount frame and deflected upwards from the test panel mounting fixture. Upon recovery of the blade on the test pad, the tip was missing and the residual length of the blade was only 36 inches.

The 24 ply panel was impacted by the upper blade with a blade release angle of 8º. The blade released cleanly from the hub and rotated about the center of gravity of the released fragment. The trajectory of the blade was approximately 4º below horizontal. The blade impacted tip first, with the length of the blade aligned with the velocity vector. The blade caused tears on both the front and back of the panel, but the tears were not aligned with one another and the blade did not penetrate through the panel. The blade deflected upwards after impact and landed on the test pad. The tip and leading edge of the blade were crushed on impact and the remaining tip and leading edge had no residual strength. The residual length of the blade was 41 inches and weighed 11.2 pounds.

Photogrammetric measurements of the backside of the 20 ply and 24 ply panels yielded measurements of the full field displacements in three directions, and the resulting in-plane strains (Ref. 2). The results provide useful data for developing and validating computational models that simulate the impact of the blade on the shielding specimens and help to explain some of the mechanisms of failure. For the 20-ply panel deflections and strains up to the point of failure were measured. More information could be obtained from results from the 24-ply panel test. At the point of maximum deflection, the 24 ply panel sustained a maximum in-plane strain of

approximately 1.5% without failure, whereas for the 20 ply panel the maximum in-plane strain was approximately 1% at the time of penetration. It was not possible with the DIC system to measure out of plane strains. The results indicate a highly dynamic event, with wave generation and fixture movement. The maximum radial displacement in the 24-ply panel is approximately 2.6 inches relative to the average displacement of four points at the corners of the specimen. The overall maximum radial displacement, including frame movement is approximately 4.3 inches. Displacements of points spanning the two cracks that formed on the back side of the specimen indicated that the crack that initiated at the fixture frame was a result of transverse tension strains, while the crack that developed in the middle of the panel initiated in a region that was displacing radially outward and was a result of transverse compression strains resulting from the dynamic wave propagation in the panel.

Summary and Conclusions

The testing described in this report validated the results of the LS-DYNA shielding design analysis (Ref. 1). The results of the testing correlate very well with the analysis results that predicted a penetration threshold between 20 and 24 plies of composite material for the open rotor composite shield impact test. In addition, the test provided data on global deformation of the composite panels and local stress concentration leading to crack initiation. The blade release in the test occurred nearly as planned except that a review of the blade trajectory determined that the blades impacted further forward than predicted due to blade rotation and aerodynamics.

Since the intent of this test was to validate the analysis, the test utilized the boundary conditions specified in the analysis. This test demonstrated that a relatively low weight solution may be possible for open rotor fuselage shielding and also validated tools that can be used to evaluate potential designs. The test also demonstrated the importance of considering local high strain effects during impact that can lead to crack initiation away from the impact site.
The numerical methods developed in Reference 1 and the experimental methods described in Reference 2 provide tools that can be used for development and validation of future open rotor fuselage shielding designs.

References

1. Carney, K., Pereira, M., Kohlman, L., Goldberg, R., Envia, E., Lawrence, C. and Roberts, G., *Weight Assessment for Fuselage Shielding on Aircraft with Open-Rotor Engines and Composite Blade Loss*, NASA/TM-2013-216582, Dec., 2013.
2. Seng, S., Frankenberger, C., Ruggeri, C.R., Revilock, D.M., Pereira, J.M., Carney, K.S. and Emmerling, W.C., Dynamic Open-Rotor Composite Shield Impact Test Report, NASA/TM-2015-218811, DOT/FAA/TC-15/22, Nov., 2015
3. Fankenberger, Chuck, and Phillips, Raena, *Open Rotor Analysis*, Naval Air Warfare Center Weapons Division Presentation, September 2012.
4. Littell, Justin, *The Experimental and Analytical Characterization of the Macromechanical Response for Triaxial Braided Composite Materials*, PhD Dissertation, U of Akron, December 2008.
5. Littell, Justin D., Binienda, Wieslaw K., Goldberg, Robert K., and Roberts, Gary D., *Characterization of Damage in Triaxial Braid Composites Under Tensile Loading*, NASA TM-2009-215645.

6. Kohlman, LeeW. *Evaluation of test methods for triaxial braid composites and the development of a large multiaxial test frame for validation using braided tube specimens*. Ph.D. Dissertation, The University of Akron, Akron, Ohio, 2012.
7. Pereira, J. Michael, Roberts, Gary D., Ruggeri, Charles, R., Gilat, Amos, and Matrka, Thomas, *Experimental Techniques for Evaluating the Effects of Aging on Impact and High Strain Rate Properties of Triaxial Braided Composite Materials*, NASA TM-2010-216763.
8. Blinzler, B.J.; Goldberg, R.K.; and Binienda, W.K.: *Macro Scale Independently Homogenized Subcells for Modeling Braided Composites*, AIAA Journal, Vol. 50, pp. 1873-1884, 2012.
9. Schweizerhof, K., K. Weimar, Th. Munz, and Th. Rottner. *Crashworthiness Analysis with Enhanced Composite Material Models in LS-DYNA – Merits and Limits.* LS-DYNA World Conference. 1998, Detroit, MI, USA.
10. Matzenmiller, J. Lubliner, and R.L. Taylor. *A constitutive model for anisotropic damage in fiber-composites.* Mechanics of Materials 20, 1995, p. 125-152.
11. Carney, K., Melis, M., Fasanella, E., Lyle, K., Gabrys, J., *Material Modeling of Space Shuttle Leading Edge and External Tank Materials For Use in the Columbia Accident Investigation*, 8th International LS-DYNA User's Conference, 2004.
12. Carney, K., Pereira, M., Revilock D., and Matheny P., *Jet engine fan blade containment using an alternate geometry and the effect of very high strain rate material behavior*, International Journal of Impact Engineering, Vol. 36, pp. 720-728, 2009.